ISSN 1070-3632, Russian Journal of General Chemistry, 2008, Vol. 78, No. 4, pp. 811–821. © Pleiades Publishing, Ltd., 2008.
Original Russian Text © A.F. Shestakov, 2007, published in Rossiiskii Khimicheskii Zhurnal, 2007, Vol. 51, No. 5, pp. 121–129.

Reactivity of Fullerene C_{60}

A. F. Shestakov

Institute of Problems of Chemical Physics, Russian Academy of Sciences,
prosp. Akad. Semenova 1, Chernogolovka, Moscow oblast, 142432 Russia
e-mail a.s@icp.ac.ru

Received February 26, 2007

Abstract—The results of a quantum-chemical study of the reactivity of fullerene C_{60} in such reactions as polymerization (dimerization), cycloaddition, addition of valence-saturated molecules are presented. The mechanisms of these reactions are also discussed.

DOI: 10.1134/S1070363208040403

INTRODUCTION

Icosahedral fullerene C_{60} is the best studied cluster representing the group of nonplanar conjugated systems. Pyramidalization of carbon atoms makes then no longer purely sp^2-hybridized and enhances reactivity of the carbon frame. According to [1], C_{60}, from the reactivity viewpoint, behaves not as an aromatic molecule, bus as an alkene with a huge electron deficite, and it can enter addition, cycloaddition, and polymerization reactions characteristic of unsaturated systems. Therefore, the reactivity of this fullerene is quite interesting to study.

Procedure for Calculation of Chemical Properties of Fullerene C_{60}

In the present work, the reactivity of C_{60} was studied by the density functional theory (DFT) method with the PBE functional [2], SBK pseudopotential [3], and extended basis sets ({3.1.1/3.1.1/1.1} for interacting atoms of the second and third periods, {5.1.1.1.1/5.1.1.1.1/5.1.1.1} for transition metals, and {3.1.1/1} for hydrogen). All calculations were performed using the PRIRODA [4]. The relative energies, unless otherwise specified, were calculated for zero temperature, including zero-point vibration energy in harmonic approximation. This approach provides correct description of the geometry and properties of C_{60}. Thus, the resulting C–C distances of 1.402 and 1.454 Å fit the experimental values 1.401(10) and 1.458(6) Å [5] obtained by gas-phase electron diffraction; the calculated wave numbers of the strongest IR vibration bands (524.5, 576.4, 1182.4, and 1450.5 cm^{-1}) are quite consistent with observations (526.7, 576.2, 1182.7, and 1429.7 cm^{-1}) [6].

Chemical Transformations of Fullerene C_{60} (Calculation Results)

Dimerization

In the crystal state, fullerenea C_{60} molecules are separated by distances of about a van der Waals contact. As the pressure is increased, the molecules get closer together and polymerize [7]. The elementary stage is bonding between neighboring C_{60} molecules in the lattice (dimerization). The activation energy of this process at $p = 1$ GPa is about 1.4 eV [8], which is close to the excitation energy of triplet excitons at this pressure. Presumably, dimerization occurs when one of the molecules is excited to a triplet state. Actually, an excited fullerene molecule is, from the chemical viewpoint, biradical and, like other radicals, can easily add to neighboring molecules by double bonds. This correlates with the known fact that optically excited C_{60} molecules dimerize and polymerize at room temperature and normal pressure [9–11]. On the other hand, with increasing pressure the forbidden band width increases thus increasing the equilibrium concentration of triplet excited states. Actually, as follows from an analysis of the reversible conductivity enhancement of single crystals of C_{60} at pressures of up to 300 kbar and the irreversible attenuation at pressures above 400 kbar [12], the decrease of the energy barrier to C_{60} polymerization with increasing

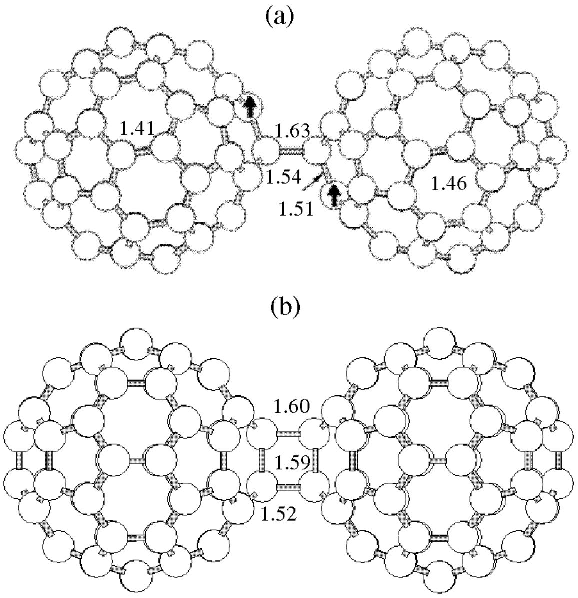

Fig. 1. Structure of triplet dimers $(C_{60})_2$ with (a) one and (b) two bridging C–C bonds, as projected on the symmetry axis. The arrows show atoms with preferential localization of the electron density. Here and hereinafter, the bond lengths are in Å.

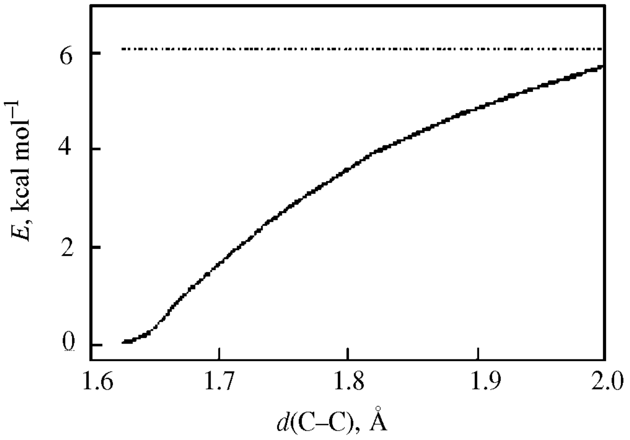

Fig. 2. Energy trend on stretching of the bridging C–C bond in the triplet $(C_{60})_2$ dimer.

pressure compares with the decrease of the forbidden band width.

Analysis of the primary addition reaction of the excited triplet C_{60} molecule to its unexcited neighbor points to thermodynamic favorability of the formation of one C–C bond between the molecules. According to calculations, this triplet adduct has an appreciably elongated C–C bond, 1.63 Å (Fig. 1a), and is formed with an energy gain of 4.3 kcal mol^{-1}. It is quite obvious that due to the quasi-free rotation about the single C–C bond, molecules need nothing mote than only come closer to each other, whereas their mutual orientation is of minor importance. It was found that the process has no activation barrier (Fig. 2). Note in this connection that exothermal reactions of radical addition to unsaturated molecules generally feature low activation energies. According to experimental and theoretical data [13, 14], hydrogen addition has a lower activation barrier than alkyl addition, since the former reaction requires no geometric deformation of one of the reactants. The above results allow the lack of energy barrier to triplet dimer formation to be explained in terms of minor changes in the geometry of the C_{60} cage; as a result, the reaction smoothly occurs as the molecules approach each other. Apparently, when the addition of any other reagent to fullerene C_{60} involves minor geometry changes, low activation energies can be expected.

A singlet dimer with one C–C bond is 2.2 kcal mol^{-1} lower than triplet and tends to cleave at the C–C bond. Interestingly, the spin density a triplet C_{60} molecule is delocalized, whereas in a triplet adduct half the spin density is localized on the two C atoms labeled by arrows in Fig. 1a. Such a spin localization creates prerequisites for formation of the most stable dimer with two bridging C–C bonds in the singlet state upon spin conversion. The corresponding energy gain is 22.1 kcal mol^{-1}. This mechanism explains the fact that the experimental activation energy of C_{60} dimerization is close to the energy of the singlet–triplet transition in C_{60}.

On the other hand, the formation of the second bridging C–C bond in the triplet adduct (Fig. 1b) requires very little energy, 3.8 kcal mol^{-1}, and, in addition, leads to localization of the spin density on one of the C_{60} molecules. Obviously, this creates conditions for fast polymerization of a crystalline fullerite C_{60}, observed on shock compression [12]. The

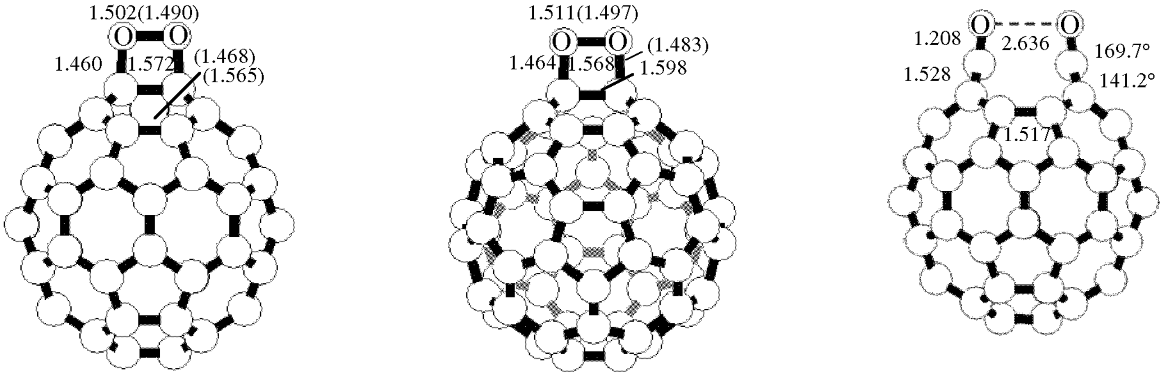

IIIa **IIIb** **IIIc**

Fig. 3. Structures of the 1,2- (**IIIa**) and 1,9-adducts (**IIIb**) of molecular oxygen with C_{60} and the transformation product $C_{58}(CO)_2$ (**IIIc**) in the singlet and triplet states. The angles between the C_3 and C_4 planes or the C–O bond and C_3 plane are shown.

geometric parameters of the $C_{60}=C_{60}$ dimer in the singlet and triplet states are almost coinciding (Fig. 1b).

Cycloaddition

An interesting possibility for reactivity research on fullerene C_{60} is provided by doped fullerites. The salting-out technique [15] allows almost complete filling of octahedral cages.

By doping with molecular oxygen, a product containing no less than 1.2 at % O_2, which corresponds to nearly half-filling of all octahedral cages, could be obtained [16]. Of important is the effect of preservation of diamagnetic properties the fullerent–oxygen adduct: Upon doping, the magnetic susceptibility changes from $-210 \pm 20 \times 10^{-6}$ to $-80 \pm 20 \times 10^{-6}$ cm^3 g^{-1}. Such a change in the magnetic susceptibility, in view of the magnetic susceptibility of gaseous oxygen ($+3440 \times 10^{-6}$ cm^3 g^{-1} [17]), suggests that these samples contain almost no paramagnetic oxygen. At the same time, oxygen in its usual paramagnetic form can be isolated from the samples. The most probable explanation for this effect [16] consists in reversible formation of a fullerent–oxygen adduct with a fairly strong chemical bonding, which changes the multiplicity of the $C_{60} + O_2$ system.

As follows from calculations, the dioxetane structure formed by the addition of O_2 across the C=C bond between two six-membered rings (1,2-addition; Fig. 3, structure **IIIa**) is stable: The energy of its formation from singlet oxygen and C_{60} is 37.1 kcal mol^{-1}. Taking into account the experimental singlet–triplet energy splitting in O_2 (22.64 kcal mol^{-1} [18]) and calculated statistic sums of the C_{60}, $C_{60}O_2$, and O_2 energies, the standard Gibbs energy of $C_{60}O_2$ formation, calculated on the assumption of a triplet ground state of O_2, is –3.2 kcal mol^{-1}. Since encapsulation in the octahedral fullerite cage should reduce the entropy of the O_2 molecule, then this calculation should provide an upper estimate for the Gibbs energy of $C_{60}O_2$ formation. The resulting value implies that the fraction of pamagnetic oxygen in the fullerene lattice is small (no more than 0.06%), which agrees with experimental magnetic data. As to the energy barrier to $C_{60}O_2$ formation, it is determined by the intercrossing field of the triplet potential energy surface for the initial $C_{60} + O_2$ system ($S = 1$) and singlet potential energy surface for the $C_{60}O_2$ adduct. Sine the triplet state of the $C_{60}O_2$ adduct, which is soin-correlated with the reagents in the ground state, in higher that the singlet state by 27 kcal mol^{-1}, then on should not expect, on a qualitative level, high activation barriers in the approximation of linear singlet–triplet term crossing. The measured activation barrier of the relative reaction of oxygen release from fullerene ozonide is 20 kcal mol^{-1} [19]. Note that the oxygen atoms in triplet $C_{60}O_2$ bear almost no spin density. Since the electronic state of triplet $C_{60}O_2$ correlates with an excited electron state of the reagents C_{60} ($S = 1$) + O_2 ($S = 0$), which creates the situation of pseudocrossing with the ground term C_{60} ($S = 0$) + O_2 ($S = 1$) and decreases the barrier to $C_{60}O_2$ formation. The corresponding triplet fullerene–singlet oxygen bonding energy is 38.6 kcal mol^{-1}.

In the calculated structure of $C_{60}O_2$ (**IIIa**), the O–O bond is appreciably “loosened,” it is longer (1.502 Å) compared with the O–O bond in triplet oxygen (1.223 Å,

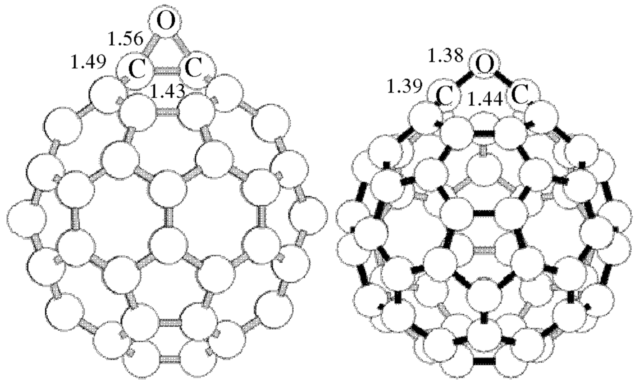

IVa **IVb**

Fig. 4. Isomeric structures of the 1,2- (**IVa**) and 1,9-adducts (**IVb**) of O with C_{60}.

experiment 1.208 Å [18]); the C–O and C–C bond lengths in the dioxetane ring are 1.460 and 1.572 Å, respectively, and the "adjacent" C–C bond lengths are 1.522 Å. The formation of the O_2 molecule much decreases the O–O vibration frequency from 1542 cm^{1} (experiment 1580 cm^{-1} [18]) to 870 cm^{-1}. However, the low intensity of this vibration, 3.0 km mol^{-1}, prevents its experimental observation.

Simultaneous O–O and C–C bond cleavage in the adduct $C_{60}O_2$ results in its transformation in the structure $C_{58}(CO)_2$ (**IIIc**) that contains two almost parallel carbonyl groups. Therewith, the energy gain is 33.6 kcal mol^{-1}. The short O–O contact (2.636 Å) between valently nonbonded atoms and the nonplanarity of conjugated five-membered carbon rings points to repulsion between the oxygen atoms, which expels the carbonyl groups from the planes defined by the three C–C(O)–C carbon atoms (deviation 10.3°). The transition state for the isomerization of **IIIa** into **IIIc** could not be localized. However, in view of the large energy gain and enlarged O–O distance in **IIIa**, we can suggest that the activation energy of fullerene–O_2 adduct formation should not be too high. This qualitative conclusion is consistent with the experimental data for C_{60} oxidation under moderate heating of oxygen-doped fullerite [16].

The isomer of $C_{60}O_2$, obtained by O_2 addition across the C–C bond between the five- and six-membered rings, 1,9 addition (adduct **IIIb**), exhibits an interesting feature: The C–C bond does not cleave, like in $C_{60}O$ isomers (Fig. 4), but elongates, like in isomer **IIIa**, but to a lesser extent (by 0.14 Å against 0.17 Å). Isomer **IIIb** is higher in energy by as little as 15.8 kcal mol^{-1} compared to basic structure **IIIa** and has a similar dioxetane ring geometry: The O–O, O–C, and C–C bond lengths are 1.511, 1.464, and 1.598 Å, respectively. The "adjacent" C–C bond lengths are 1.489 and 1.517 Å in the six- and five-membered rings, respectively. The other C–C bond lengths in C_{60} vary no more than 0.01 Å. The singlet–triplet energy splitting in **IIIb** is smaller (10.0 kcal mol^{-1}).

In view of the fact that the formally double and formally single bonds in fullerene C_{60} behave similarly in O_2 addition, we studied the structures of isomeric ozone adducts with C_{60} to find that they have similar structures (Fig. 5). Therewith, in view of the nonplanarity of the C_2O_3 ring, the 1,9 addition across the C–C bond gives rise to two conformers **Vb** and **Vc** with close ozone bond energies (21.5 and 19.1 kcal mol^{-1}, respectively). The most stable 1,2 isomer **Va** is formed with an energy gain of 34.4 kcal mol^{-1}. Upon ozone addition, the O–O bonds get longer by 0.17 Å, while the O–O–O (101°) gets smaller than in the ozone molecule (118°). Because of this angle distortion, even though the energies of O_2 and O_3 addition across the C–C bond are close to each other, the C–C bond in the oxygen adducts is longer by about 0.05 Å than in the ozone adducts. Note that the oxygen fragments in the considered $C_{60}O_n$ molecules accept almost equal electron densities: –0. 41 (**a**), –0,45 (**b**) ($n = 1$), and –0.50 ($n = 2, 3$).

According to calculations, the reaction of the HO_2 radical and C_{60} results in chemical bonding [d(C–O) = 1.45 Å, (O–O) = 1.47 Å] with an energy gain of 8.5 kcal mol^{-1}. Abstraction of the hydroperoxide H atom formally leads to a complex of a triplet oxygen molecule with fullerene, containing one C–O bond. However, the calculations show that the structure of the complex corresponds to a weakly bound van der Waals complex. In a similar way, the NO molecule possessing one unpaired electron forms with fullerene only a weakly bound van der Waals adduct. However, simultaneous addition of two NO molecules in the 1 and 4 positions forms a chemically bound structure with low energy expenses, 3.7 kcal mol^{-1} (Fig. 6, structure **VIa**). In the case of 1,2 addition which should provide the most energetically favorable structure, the system proves unstable with respect to N–N bond formation (structure **VIb**). Therewith, the bond energy of two NO molecules is 18.4 kcal mol^{-1}. In the isomeric 1,9-adduct containing a four-membered ring (structure **VIc**), the bond energy is lower (3.2 kcal mol^{-1}).

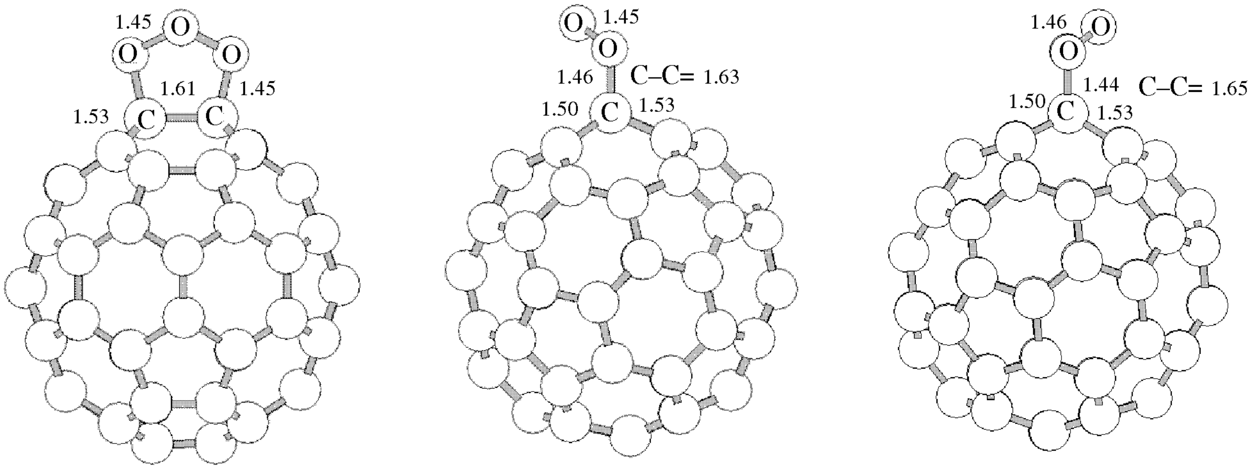

Va **Vb** **Vc**

Fig. 5. Isomeric structures of 1,2- (**Va**) and 1,9-adducts (**Vb, Vc**) of ozone with C_{60}.

These results allow a preliminary conclusion that appropriate azo compounds can readily add to fullerenes. Comparison of isomeric products of addition of various substrates to C_{60} across the C–C bond reveals a certain regularity: The energy gain on 1,2 addition proves about 15 kcal mol^{-1} larger than on 1,9 addition.

In the considered $C_{60}N_2O_2$ molecules, N–O vibrations are very intense and, therefore, readily observable. The wave numbers of symmetric N–O vibrations in structures **VIa**, **VIb,** and **VIc** are 1660 (1571) 1555 (128), and 1543 cm^{-1} (549), and those of antisymmetric N–O vibrations are 1641 (882) 1530 (213), and 1528 cm^{-1} (128), respectively (parenthesized are intensities in km/mol). There are also highly intense N–N vibrations in structures **VIb** [1568 cm^{-1} (368)] and **VIc** [1547 cm^{-1} (295)].

In adduct **VIa,** there is almost no NO–C_{60} charge transfer. At the same time, upon N–N bond formation the N_2O_2 fragment acquires a negative charge of –0.22 e. This finding and the fact that the N–N bond length (1.36 Å) is close to a double-bond length allows structures **VIb** and **VIc** to be considered as di-*N*-oxides of ozone adducts with fullerene. The calculated mean

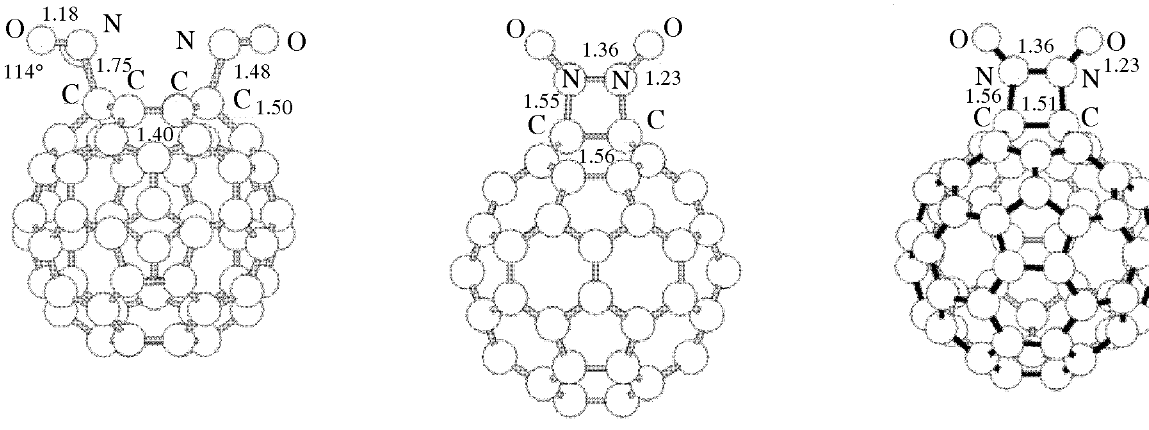

VIa **VIb** **VIc**

Fig. 6. Isomeric structures of 1,4- (**VIa**), 1,2- (**VIb**, and 1,9-adducts (**VIc**) of two NO molecules with C_{60}.

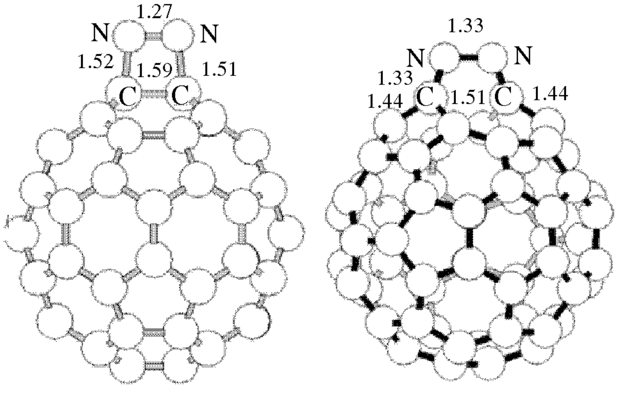

VIIa **VIIb**

Fig. 7. Isomeric structures of 1,2-adducts of N_2 with C_{60}, formed with cleavage (**VIIa**) and without cleavage (**VIIb**) of the C–C bond.

bond energy of the oxygen atoms in **VIb** is quite high (84.4 kcal mol^{-1}). However, when appropriate reducers are used, the formation of azo derivative **VIIa** (Fig. 7) becomes an energetically favorable process. The decomposition of **VIIa** into nitrogen and fullerene is accompanied by an energy gain of 62.2 kcal mol^{-1}. It is not quite understandable why its isomer **VIIb** with a cleaved C–C bond (analog of **IIIc**) is, against expectations, is even more unstable and is higher in energy by 24.5 kcal mol^{-1}.

Addition of Valence-Saturated Molecules

Fullerenes not only enter addition and cycloaddition reactins with active reagents, but can also take up valence-saturated molecules, such as alkanes (methane inclusive) [20]. We performed a theoretical analysis of such addition reactions with CH_4, NH_3, and H_2O as reagents. In terms of the heat effect, 1,2-additions of CH_4, NH_3, and H_2O are nearly thermally neutral reactions. According to calculations, the respective energy expenses are 0.7, 5.7, and 4.8 kcal mol^{-1}. The structures of the transition states of these reactions are shown in Fig. 8. As judged from the degree of elongation of the bond being cleaved, we deal here with early (reagent-like) transition states. The activation energies are moderate: 34.0 (NH_3) and 39.6 (H_2O) kcal mol^{-1}, except for that for the reaction with CH_4 (77.1 kcal mol^{-1}). Such a high barrier corresponds to temperatures above 600°C, at which methane undergoes catalytic transformation in the presence of fullerenes [20]. Noteworthy, the molecule to be added imparts an appreciable part of its electron density to the fullerene molecule. Therewith, the charge on H_2O (+0.21), NH_3 (+0.35), or CH_4 (+0.41) correlates both with the total elongation of the cleaving bond and the bond formed with the participation of H and with the H–C distance to the closest C atom. This points, on the one hand, to enhancing donor power of H in the above series and, on the other, to enhancing interaction with the carbon cage as a result of enhancing charge transfer.

For the sake of comparison, we considered additions of H_2O to all-*trans*-1,3,5-triene

$$C_2H_3CH{=}CHC_2H_3 + H_2O = C_2H_3CH_2CHOHC_2H_3 - 5.2 \text{ kcal mol}^{-1}$$

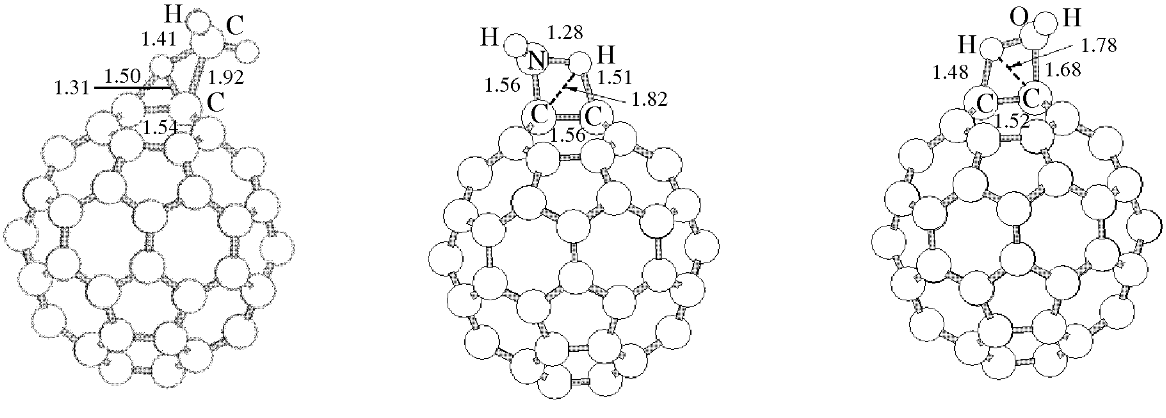

VIIIa **VIIIb** **VIIIc**

Fig. 8. Structures of four-membered transition states of addition of CH_4 (**VIIIa**), NH_3 (**VIIIb**), and H_2O (**VIIIc**) to C_{60}. The H atoms of symmetrically located C––H (**VIIIa**) and N–H (**VIIIb**) bonds are projected to each other.

and benzene

$$C_6H_6 + H_2O = 1{,}2\text{-}C_6H_7OH - 23.8\ \text{kcal mol}^{-1}.$$

In both cases, higher, compared to fullerene, activation barriers were obtained (4.1 and 17.4 kcal mol^{-1}, respectively). Thus, in similar, in terms of thermodynamics, water addition reactions to the polyene and fullerene C_{60}, the latter is more reactive.

The theoretical analysis of water addition to ethylene [21] shows that inclusion of an additional water molecule makes it possible to pass from an unfavorable four-membered transition state to six-membered, which reduces the energy barrier to be reduced by about 20 kcal mol^{-1}. This possibility was explored on an example of fullereney C_{60}. Inclusion of an additional H_2O or NH_3 molecule allows concerted addition through a six-membered transition state (Fig. 9). In this case, the activation energy gets much lower (19.7 kcal mol^{-1}), and the reaction can occur in mild conditions. In the case NH_3 addition involving a molecule of H_2O (structure **IXb**) or NH_3 (**IXc**), a still stronger reduction of the energy barrier is observed: to 13.8 and 13.7 kcal mol^{-1}, respectively. Counting not from the energies of free molecules, but from the total energy of C_{60} and the corresponding dimer, and including the H-bond energy (~5 kcal mol^{-1}), the activation energies of concerted addition of water and ammonia can be estimated at 19–24 kcal mol^{-1}. This result suggest that valence-unsaturated molecules can add to fullerene in the absence of photochemical activation of the latter.

The charges accepted by fullerene are–0.29, –0.35, and –0.46 for from structures **IXa**, **IXb,** and **IXc,** respectively. The fairly strong charge transfer explains the increase of the coordination number in these structures to 3 in O and to 4 in N, like in oxonium and ammonium ions, respectively; this increase is accompanied by the appearance of a double-bonded hydrogen, like in proton solvates. This is a probable reason for the appreciably reduced activation barrier for concerted addition of H_2O and NH_3 to fullerene. Note that concerted addition of water to ethylene which possesses no acceptor properties involves no increase of the coordination number of the O atom [21].

In a more complicated case, isopropanol addition to fullerene, similar results were obtained. Two alcohol molecules form an H-bonded dimer $(CHMe_2OH)_2$ with an energy gain of 5.1 kcal mol^{-1}. The H···O hydrogen bond length is 1.89 Å, and O–H···O group is almost linear: The O–H···O angle is 174°. The structure of the six-membered transition state of the concerted addition of $CHMe_2OH$ to fullerene is shown in Fig. 10 (structure **Xa**). The structure contains an O atom with two O–H bonds and having the coordination number 3. Analysis of the electron density distribution shows that the charge on the H_2OCHMe_2 group is +0.29, and the charge on the transferred hydrogen atom is +0,37 which is higher than the charge (+0.30) on the mobile hydrogen atom in isopropanol. The total charge transfer on the fullerene molecules is –0.33.

The activation energy is 22.5 kcal mol^{-1} relative C_{60} + $(CHMe_2OH)_2$, which suggests an appreciable fullerene

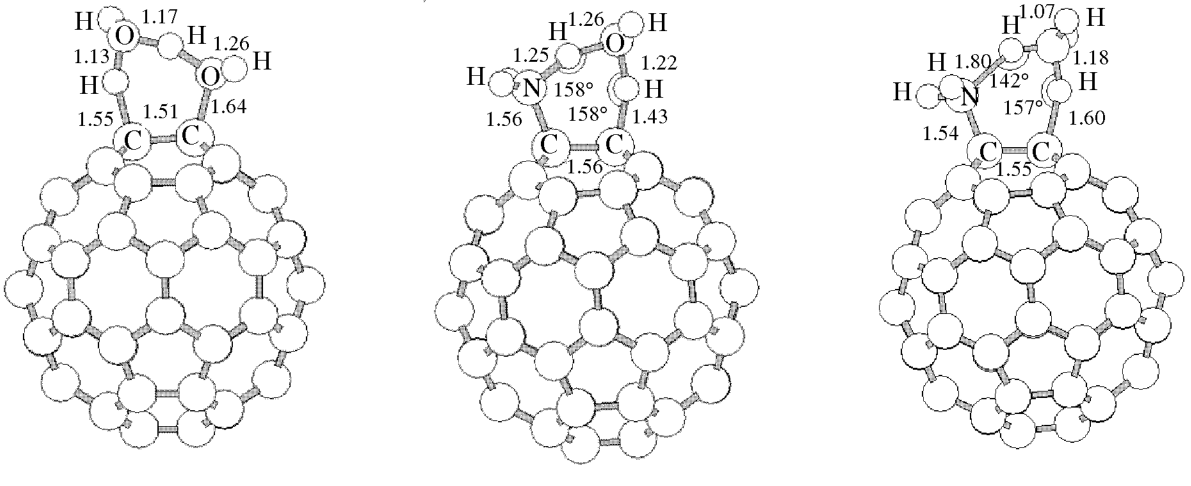

IXa **IXb** **IXc**

Fig. 9. Structures of six-membered transition states of addition of H_2O (**IXa**) and NH_3 (**IXb, IXc**) to C_{60}.

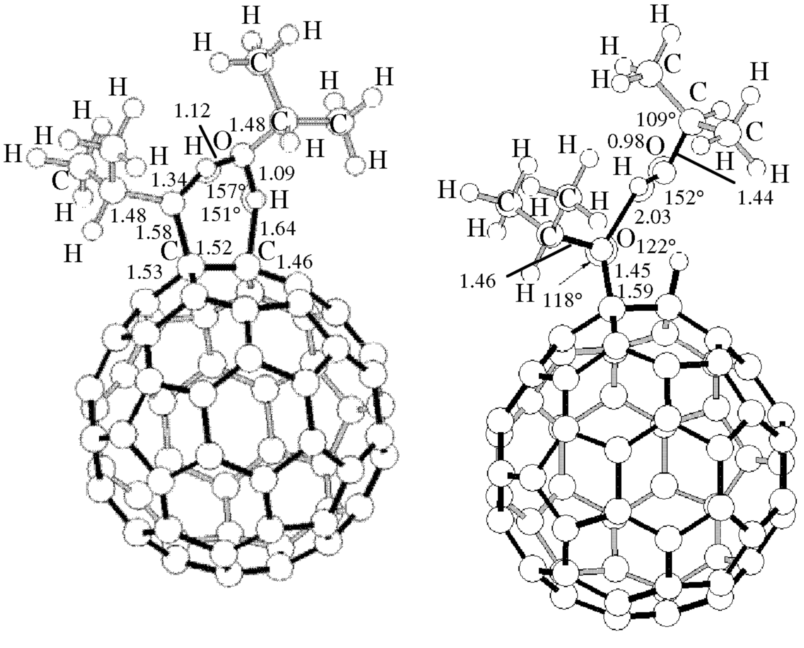

Xa **Xb**

Fig. 10. Structures of transition state **Xa** and adduct **Xb** of isopropanol with C_{60}.

reactivity, since the reaction is only slightly endothermic and requires 7.4 kcal mol^{-1} to proceed. Comparison of the structure of product **Xb** with the structure of the starting isopropanol dimer points to certain steric hindrances: The C–O–C (118°) and H–O–C (122°) angles of the added isopropanol residue in **Xb** are larger than their respective angles (108° and 110°) in the starting alcohol dimer. This eventually results in the elongation of the hydrogen bond between the alcohol molecules to 2.03 Å and in the decrease in its energy to 3.7 kcal mol^{-1}. This, the 1,2 addition of isopropanol to C_{60} can occur in mild conditions. The decomposition of $CHMe_2OH$ into acetone and hydrogen is an endothermic process. However, the decomposition of the isopropanol 1,2-addition product into acetone and fullerene 1,2-dihydride is already an exothermic reaction:

$$C_{60}OCHMe_2(H) = C_{60}H_2 + OCMe_2 + 7.3 \text{ kcal mol}^{-1}$$

Consequently, there are all grounds to believe that the decomposition of isopropanol in the presence of fullerene occurs at a lower temperature.

To gain insight into the mechanism of this process, we chose the model reaction of the decomposition of the radical adduct

$$C_{60}OCHMe_2 = C_{60}H + OCMe_2 + 8.9 \text{ kcal mol}^{-1}.$$

The structure of the five-membered transition state is shown in Fig. 11 (structure **XIa**). The activation barrier is 15.8 kcal mol^{-1}. The moderate activation energy is a consequence both of the concentration of an essential spin density (46%) on the neighboring carbon atom along the bond between two hexahedrons in the $C_{60}OCHMe_2$ radical and the low bond energy of the alkoxy group (21.1 kcal mol^{-1}). The spin density on the respective C atom in the $C_{60}H$ radical is close to this value (43%). The spin density in the transition state is mostly concentrated on the carbonyl carbon atom (48%).

The adduct of isopropanol with one fullerene molecule is a system with filled electron shells. Therefore, the hydrogen transfer to the C_{60} carbon frame during decomposition of the adduct will not involve a large spin density, which should increase the activation energy.

For illustration we considered, of all possible cases, the decomposition of the 1,9-isomer of hydroalkoxyfullerene which is higher by 14.9 kcal mol^{-1} than the major 1,2-isomer. The transition state (structure **XIb**) is later than in the previous case (more product-

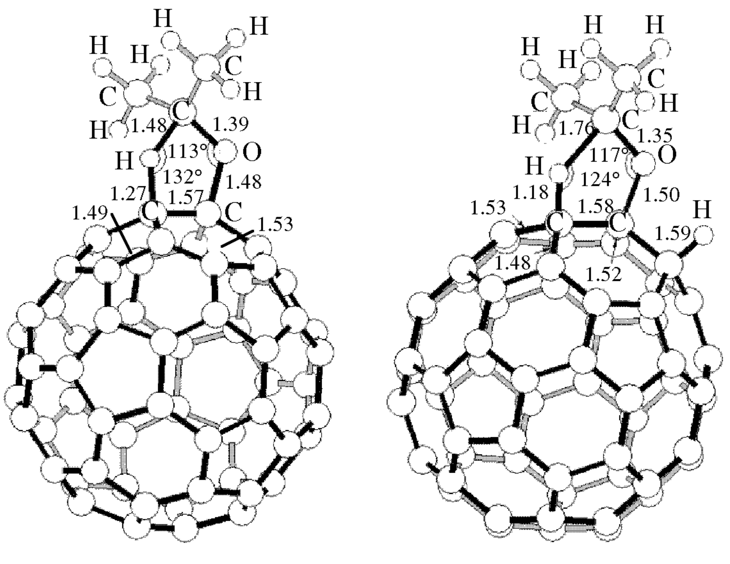

XIa **XIb**

Fig. 11. Structures of the transition states of the decomposition of $C_{60}(OCHMe_2)$ (**XIa**) and $C_{60}(OCHMe_2)(H)$ (**XIb**) with acetone formation.

like), as would be expected, since this reaction occurs with , whose product is the minor 1,3-isomer of $C_{60}H_2$ (it is higher by 33.9 kcal mol^{-1} of the major 1,2-dihydrofullerene isomer, requires energy (11.7 kcal mol^{-1}) to occur. The activation energy is moderate (28.1 kcal mol^{-1}). The principal difference between **XIb** and **XIa** consists in an unsymmetrical distortion of the carbon frame about the C–C bond incorporated in the five-membered ring involving the transferred hydrogen. While not providing an exhaustive picture of the reaction of isopropanol with fullerene, the above findings explain, on a qualitative level, the appearance of acetone on moderate heating of C_{60} intercalated with isopropanol at tetemperatures above 200°C [22].

Formation of π Complexes

Fullerene can also function as a π-type ligand in transition metal complexes [23]. It can be suggested that the incorporation of C_{60} in the coordination sphere of a metal complex (provided a vacancy is available) should occur with a low activation barrier. In this connection of interest is the complex $Mo(dppe)_2(N_2)_2$ (dppe = $PPh_2C_2H_4PPh_2$) whose dinitrogen ligand is known to be quite labile and can be easily substituted by other ligands [24]. It can be expected that the dinitrogen ligand can be substituted by fullerene. Note that quasioctahedral Mo and W complexes containing two fullerene ligands are known [25]. DFT calculations reasonably reproduce the structure of the starting $Mo(dppe)_2(N_2)_2$ complex [26], and the calculated wave numbers nicely fit experimental (in parentheses) for symmetrical 2042 (2036) cm^{-1} and antisymmetrical 1992 (1976) cm^{-1} vibrations of the N–N bond.

To simplify calculations of fullerene-containing systems, as model complexes we took structures in which all phenyl groups in the dppe ligand are substituted by H. In this case, the geometric parameters and N–N vibration wave numbers (2072 and 2038 cm^{-1}) of the starting dinitrogen complex vary only slightly.

The calculated bond energies of N_2 (31.7 kcal mol^{-1}) and C_{60} (28.1 kcal mol^{-1}) in the model complexes Mo$(PH_2C_2H_4PH_2)_2(N_2)_2$ and $Mo(PH_2C_2H_4PH_2)_2(N_2)(C_{60})$ (Fig. 12, structure **XIIa**) prove quite close to each other. This fact suggests that the substitution of nitrogen by fullerene in the dinitrogen complex is almost thermally neutral. However, taking into account that the translational energy of the nitrogen molecule contributes much into the entropy, the Gibbs energy of the incorporation of C_{60} in the coordination sphere, attended with release of gaseous N_2, proves to be below zero, and this is the driving force of the reaction.

As the fullerene molecule enters the coordination sphere of the full complex, the character of bonding of the dppe ligand changes because of the insufficient place available for accommodation of bulky phenyl groups. As a result, the Mo–P bonds get longer by, on

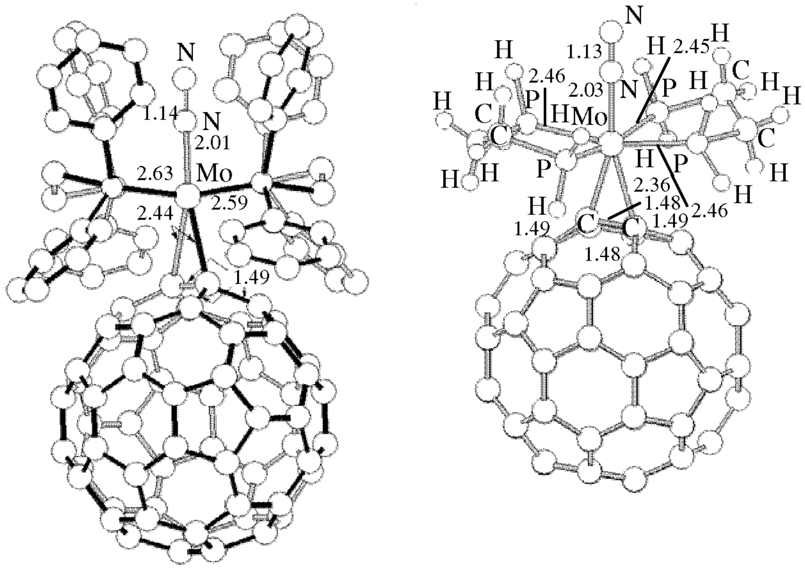

XIIa **XIIb**

Fig. 12. Structures of the complexes $Mo(PH_2C_2H_4PH_2)_2(N_2)(C_{60})$ (**XIIa**) and $Mo(dppe)_2(N_2)(C_{60})$ (**XIIb**).

average, 0.15 Å, which affects the donor–acceptor properties of the coordination center, shortens the Mo–N distance, and elongates the N–N distance. Therewith, the Mo–C distances increase by 0.08 Å, but, however, the coordination C–C bond, too, gets longer. Together these findings suggest that the molybdenum center exerts a stronger effect on the dinitrogen and fullerene ligands. Even though the geometric characteristics of the coordination of nitrogen in the model and full complexes are close to each other, the bond energies of the N_2 ligand are quite different: 26.7 and 7.0 kcal mol^{-1}, respectively. The lower bond energy in the latter complex can be associated with shortened N…H contacts (up to 2.5 Å) with phenyl hydrogen atoms, which destabilize the system. On the other hand, upon N_2 release the complex undergoes a fairly strong structural rearrangement: Mo–N, Mo–C, and Mo–P binds shorten to 2.30, 2.51, and 2.54 Å, respectively, which should be accompanied by an energy gain.

However, the calculated ligand bond energies in the $Mo(dppe)_2(N_2)(C_{60})$ complex should be considered with caution. The case in point is that this system involves a lot of intramolecular van der Waals contacts, including those between the dppe benzene rings and C_{60}, which reach 3.1 Å. Therefore, van der Waals interactions in the vicinity of these contacts and their changes on the rearrangement of the system should contribute much into the molecular energy. As known, standard DFT methods do not explicitly include dispersion interactions but only mimic them. Therefore, the correct bond energy between the dinitrogen and fullerene ligands in the $Mo(dppe)_2(N_2)$ (C_{60}) and $Mo(dppe)_2(C_{60})_2$ complexes is still unknown. Note that to overcome this drawback of the DFT method, new combined approaches are being presently developed [27, 28] for more correct description of nonvalence interactions.

Thus, our present study shows that fullerene C_{60} can react by different mechanisms in mild conditions.

REFERENCES

1. Amal, S. and Sahoo, S.K., *Bull. Mat. Sci.*, 1997, vol. 20, p. 141.
2. Perdew, J.P., Burke, K., and Ernzerhof, M., *Phys. Rev. Lett.*, 1996, vol. 77, p. 3865.
3. Stevens, W.J., Basch, H., and Krauss, M., *J. Chem. Phys.*, 1984, vol. 81, p. 6026.
4. Laikov, D.N., *Chem. Phys. Lett.*, 1997, vol. 281, p. 151.
5. Bethune, D.S., Meijer, G., Tang, W.C., Rosen, H.J., Golden, W.G., Seki, H., Brown, C.A., and de Vries, M.S., *Ibid.*, 1991, vol. 179, p. 181.
6. Li, X.D., Cheng, W.D., Wu, D.S., Zhang, H., Gong, Y.J., and Lan, Y.Z., *Ibid.*, 2003, vol. 380, p. 480.
7. Davydov, V.A., Kashevarova, L.S., Rakhmanina, A.V., Dzyabchenko, A.V., Senyavin, V.M., and Agafonov, V.N., *Ross. Khim. Zh.*, 2001, vol. 45, no. 4, p. 25.
8. Davydov, V.A., Kashevarova, L.S., Rakhmanina, A.V., Senyavin, V.M., Pronona, O.P., Oleynikov, N.N.,

Agafonov, V., Ceolin, R., Allouchi, H., and Szwarc, H., *Chem. Phys. Lett.*, 2001, vol. 333, p. 224.

9. Rao, A.M., Ping, Z., Kai-An, W., Hager, G.T., Holden, J.M., Ying, W., Lee, W.T., Xiang-Xin, Bi, Eklund, P.C., Cornett, M.A., Duncan, M.A., and Amster, I.J., *Science,* 1993, vol. 259, p. 955.
10. Sekar, C., Thamizhavel, A., and Subramanian, C., *Physica C*, 1997, vol. 275, p. 193.
11. Manika, I., Maniks, J., and Kalnacs, J., *Fullerene Sci. Tech.*, 1997, vol. 5, p. 149.
12. Osip'yan, Yu.A., Avdonin, B.V., Kagan, K.L., Nikolaev, R.K., Postnov, V.I., Sidorov, N.S., Shahrai, D.V., Shestakov, A.F., Kveder, V.V., and Fortov, V.E., *Pis'ma v ZhETF*, 2005, vol. 81, p. 587.
13. Shestakov, A.F., Denisov, E.T., and Emel'yanova, N.S., *Izv. Akad. Nauk, Ser. Khim.*, 2005, p. 886.
14. Denisov, E.T., Shestakov, A.F., and Emel'yanova, N.S., *Kinet. Katal.*, 2006, vol. 47, p. 669.
15. Shul'ga, Yu.M., Martynenko, V.M., Baskakov, S.A., Skokan, E.V., Arkhangelskii, I.V., Schur, D.V., and Pomytkin, A.P., Proc. VIII Int. Conf. *"Hydrogen Material Science and Chemistry of Metal Hydrides",* Sudak, Crimea, Ukraine, September 14–20, 2003, p. 582.
16. Shul'ga, Yu.M., Martynenko, V.M., Shestakov, A.F., Baskakov, S.A., Vasilets, V.N., and Morozov, Yu.G., *Izv. Akad. Nauk., Ser. Khim.*, 2006, p. 662.
17. *Khimicheskaya entsiklopediya* (Chemical Encylpaedia), Moscow: Sovetskaya Entsiklopediya, 1990, vol. 2, p. 387.
18. Huber, K.-P. and Herzberg, G., *Constants of Diatomic Molecules,* New York: Reinhold, 1979.
19. Heymann, D., Bachilo, S.M., Weisman, R.B., Cataldo, F., Fokkens, R.H., Nibbering, N.M.M., Vis, R.D., and Chibante, L.P., *J. Am. Chem. Soc.*, 2000, vol. 122, p. 11473.
20. Gol'dshleger, N.F. and Moravskii, A.P., *Usp. Khim.,* 1977, vol. 66, p. 353.
21. Pokidova, T.S., Denisov, N.T., and Shestakov, A.F., *Neftekhimiya*, 2007, in press.
22. Shul'ga, Yu.M., Martynenko, V.M., Shestakov, A.F., Baskakov, S.A., Knerel'man, E.I., Mu-rav'ev, D.N., Open'ko, V.V., and Horkin, E.E., *Izv. Akad. Nauk. Ser. Khim.*, 2007, in press.
23. Neretin, I.S. and Slovokhotov, Yu.L., *Usp. Khim.*, 2004, vol. 73, p. 492.
24. Sato, M., Taysumi, T., Kodama, T., Hidai, M., Uchida, T., and Uchida, Y., *J. Am. Chem. Soc.*, 1978, vol. 100, p. 4447.
25. Jin, X., Xie, X., and Tang, K., *Chem. Commun.*, 2002, p. 750.
26. Zeller, M. and Hunter, A.D., *Z. Kristallogr. NCS*, 2004, vol. 219, pp. 249–254.
27. Lundqvist, B.I., Chakarova-Kack, S., Cooper, V.R., Dion, M., Hyldgaard, P., Kleis. J., Li Shen, Langreth, D.C., Puzder, A., Rydberg, H., Schroder, E., Simac, S., and Thonhauser, T., Abstracts of Papers, *12th Int. Conf. on the Applications of Density Functional Theory in Physics* and *Chemistry*, August 26-30, 2007, Amsterdam, p. 17.
28. Jansen, G. *Ibid*, p. 18.